

ORIGINAL ARTICLE

Quantification of compaction-induced crystallinity reduction of a pharmaceutical solid using ^{19}F solid-state NMR and powder X-ray diffraction

Jodi Liu, Karthik Nagapudi, Y.-H. Kiang, Ezequiel Martinez and Janan Jona

Small Molecule Pharmaceutical R&D, Amgen Inc., One Amgen Center Drive, Thousand Oaks, CA, USA

Abstract

^{19}F solid-state nuclear magnetic resonance (NMR) was investigated as an analytical technique to quantify the amorphous phase in a fluorine-containing pharmaceutical candidate. The crystallinity of Compound 1 was calculated using two ^{19}F T_1 relaxation-based methods. The first method employs both the pure amorphous and the crystalline reference standards while the second method is model independent and utilizes a single standard. The ^{19}F solid-state NMR results were confirmed with powder X-ray diffraction methods. From X-ray diffraction data, two linear calibration curves were obtained from blends of crystalline and amorphous Compound 1: one is based on the total integrated intensity of selected diffraction peaks and the other on the total intensity of the amorphous halo at 2θ positions that have no interference from crystalline diffraction peaks. The crystallinity of Compound 1 after compaction calculated by both ^{19}F solid-state NMR methods was in excellent agreement with the results from the X-ray calibration curves. ^{19}F solid-state NMR was shown to be a powerful technique in determining the amount of amorphous phase present in a pharmaceutical solid.

Key words: *Compaction-induced amorphization; ^{19}F solid-state NMR; model-independent method; quantification of amorphous content; XRD*

Introduction

The majority of active pharmaceutical ingredients used in solid dosage formulations are crystalline solids. The crystalline state is a thermodynamically stable state compared to the disordered amorphous state, in which the geometry and symmetry are frustrated at the molecular level¹. Although the amorphous state is thermodynamically unstable and in theory will eventually relax and crystallize, kinetically stable amorphous forms can be induced by various processes and can coexist with the crystalline phase for a variable period of time². Common pharmaceutical processes that may induce amorphization include milling, grinding, desolvation, and compaction^{3–6}. The higher free energy of the amorphous form often results in higher solubility, dissolution rate, hygroscopicity, and solid-state reactivity that may in turn affect the performance of the solid dosage formulation^{1,4,7,8}. It is

therefore important to monitor and control the amount of amorphous phase formed during processing. The most widely marketed solid dosage form is a tablet. As compaction can induce amorphization, it is necessary to examine the crystallinity of compacted drug substances in the early stages of solid dosage formulation development. If reduction in crystallinity is observed after compaction, quantification of the amount of amorphous phase is critical for quality and process control.

Among various analytical techniques that have been used for quantitation of the amorphous phase in pharmaceutical solids, powder X-ray diffraction (XRD) has been one of the most widely attempted because of the accessibility of instrumentation in laboratories, relative simplicity, short data collection time, and its capability of direct detection of molecular order or lack thereof in solids⁹. However, disadvantages of using quantitative XRD include microabsorption, preferred orientation, complex

Address for correspondence: Y.-H. Kiang, Small Molecule Pharmaceutical R&D, Amgen Inc., One Amgen Center Drive, Thousand Oaks, CA 91320, USA.
E-mail: ykiang@amgen.com

(Received 21 Jul 2008; accepted 5 Jan 2009)

ISSN 0363-9045 print/ISSN 1520-5762 online © Informa UK, Ltd.
DOI: 10.1080/03639040902729424

<http://www.informapharmascience.com/ddi>

scattering patterns, and incompatibility with excipients. In addition, careful sample preparation and large sample sizes are generally required for XRD methods. Though other techniques do not directly 'see' the molecular packing in solids as XRD does, they may provide other various advantages over diffraction methods in quantifying amorphous content^{10,11}. A combination of methods is useful in determining the accuracy of the quantitation results.

Solid-state nuclear magnetic resonance (NMR) is becoming increasingly important in the characterization of pharmaceutical solids^{12,13}. Most crystallinity quantification work done to date in the pharmaceutical field has concentrated on applications of ¹³C solid-state NMR, as carbon is one of the most ubiquitous nuclei in drug substances^{14–16}. ¹³C-based quantitation methods have relied on either least squares type analysis or measurement of relaxation parameters to be used in combination with peak areas. Gustafsson et al.¹⁴ and Lefort et al.¹⁵ used least squares analysis to estimate the amount of the amorphous phase in mixtures containing both amorphous and crystalline phases. This method requires both amorphous and crystalline standards. Offerdahl et al.¹⁶ measured the relaxation constants pertinent to cross polarization experiments and used this information in combination with the integrated peak area of selected chemical shifts to estimate the amount of different neotame polymorphs present in a sample. This method is attractive as it does not require standards if the ¹³C spectrum shows sufficient chemical resolution.

With medicinal chemists routinely incorporating fluorine atoms in development candidates to increase permeability, the ¹⁹F nucleus has become more available for pharmaceutical solid-state NMR characterization work¹⁷. The high gyromagnetic ratio and 100% natural abundance of ¹⁹F allow for high sensitivity that is required to quantify low amorphous content or to investigate low drug load formulations. It has also been shown that ¹⁹F solid-state NMR is exceptionally powerful in distinguishing amorphous and crystalline forms in both bulk and formulation samples¹⁷. Using the ¹⁹F nucleus can be advantageous over the more common ¹³C nucleus in oral formulations as excipient components also contribute to the ¹³C spectrum. In addition, the required sample size is typically smaller than that required by techniques such as powder XRD. Despite the advantages offered by ¹⁹F solid-state NMR, the utilization of ¹⁹F nuclei for crystallinity quantification in pharmaceutical solids has been scarce if not absent from literature.

In this work, the crystallinity reduction of a pharmaceutical development compound after compaction was quantified using ¹⁹F solid-state NMR. In principle, any of the quantitative ¹³C-based methods discussed earlier can be applied to ¹⁹F-based quantitation. However, unlike ¹³C because of the 100% natural abundance of ¹⁹F, cross polarization is typically not necessary for the

¹⁹F nucleus, which makes quantitation much more straightforward. In this work, two ¹⁹F solid-state NMR methods were used: one is based on utilizing two reference standards and the other based on a single standard approach. Both methods directly exploit the spin lattice relaxation time (T_1) difference between the crystalline and amorphous phases, which is not practically applicable to ¹³C solid-state NMR because of the low sensitivity of ¹³C nucleus and the necessity of cross polarization. The single standard approach uses a simple T_1 filter experiment to selectively monitor the signal from either the crystalline or the amorphous phase. This selected signal can then be directly related to the amount of the phase being observed as ¹⁹F-based experiments are fully quantitative. In addition, the single standard method is more robust to day-to-day instrument fluctuations and to improperly calibrated pulses. To our knowledge, this method has not been exploited in pharmaceutical literature for the quantitation of phases. This work demonstrates the quantification of compaction-induced crystallinity reduction by applying ¹⁹F solid-state NMR technology. The accuracy of the ¹⁹F NMR quantification is confirmed with the more established analytical technique of powder X-ray diffraction.

Experimental section

Materials

Crystalline and amorphous Compound 1 were obtained from the Chemistry Process Research and Development Department of Amgen Inc. (Thousand Oaks, CA, USA) with greater than 98% purity. Hexane was purchased from Aldrich (Milwaukee, WI, USA) and was used without further purification. The received crystalline Compound 1 material is assumed to be 100% crystalline and the amorphous Compound 1 is assumed to be 0% crystalline.

Sample preparation

Appropriate amounts of 100% and 0% crystalline Compound 1 were weighed out to generate standard curves. The amorphous material was ground with a mortar and pestle prior to mixing. Mixing and further particle size homogeneity were achieved by slurring each parent material or blending with hexane at ambient temperature. The slurries were filtered, dried over nitrogen, and passed through a 200-mesh sieve. To ensure that recrystallization or change of crystallinity of Compound 1 in hexane had not occurred, the supernatant of the hexane slurry was analyzed for its Compound 1 level using high-performance liquid chromatography (HPLC).

A Carver hydraulic press and a flat-faced die set of 5 mm diameter were used to prepare 100-mg tablets of

crystalline Compound 1. The tablets were compacted to 566 MPa with a dwell time of 20 seconds. For crystallinity measurements, tablets were crushed with a spatula and sieved through a 200-mesh sieve.

¹⁹F solid-state NMR

The ¹⁹F solid-state NMR experiments were performed on a Brüker DSX-500 MHz NMR spectrometer using a Brüker 4-mm double resonance broadband MAS probe. The samples for ¹⁹F NMR experiments were packed in 4-mm zirconia rotors with vespel endcaps and a spinning speed of 14 kHz was employed for all measurements. A $\pi/2$ pulse length of 4 μ s and a recycle delay of 15 s were employed for all measurements. Depending on the experiment, 32–64 transients were collected for signal averaging. ¹⁹F T_1 relaxation data were obtained using a standard inversion recovery pulse sequence with a π pulse length of 8 μ s. All spectra were referenced to poly(tetrafluoroethylene) (Teflon®), which was assigned to a chemical shift of –122 ppm.

For the two-reference method, pure crystalline and pure amorphous relaxation data were fitted to the monoexponential equation $I = I_0 + p \cdot e^{-t/T_1}$, where I_0 , p , and T_1 are the parameters to be fitted to obtain the T_1 relaxation of the pure materials. Using the T_1 relaxation times and constants obtained from the pure crystalline and amorphous fits (I_0 , T_{1c} , p_c , T_{1a} , p_a), crystallinity of the crushed tablets was determined by fitting the experimental relaxation data to the biexponential equation

$I = I_0 + \alpha p_c \cdot e^{-t/T_{1c}} + (1 - \alpha) e^{-t/T_{1a}}$, where α is the crystallinity to be fitted. For the single standard method, the ¹⁹F resonance peak at a delay time $\tau = 1.31$ s was directly integrated.

X-ray diffraction

Powder patterns were recorded with a PANalytical X'Pert PRO X-ray powder diffractometer equipped with a multiple-wire-type detector. The diffractometer employs Ni-filtered Cu K α radiation at 45 kV, 40 mA, a divergence slit of 1/4°, and an antiscatter slit of 1/2°. The samples were analyzed with a step size of 0.0084° and sampling time of 0.674 seconds per step. The calibration and performance of the instrument was checked daily using NIST Silicon standard SRM 640c.

A backloading sample holder of 16 mm diameter and 2.4 mm depth was used to ensure consistent packing and sample volume. The holder was placed against a stand with a level surface, and the powder sample was filled from the back, such that the powder surface was flat and flush with the front of the holder. For each sample, the X-ray diffraction was measured in triplicate, and the sample was repacked and newly mounted for each measurement.

The powder patterns were fitted to pseudo-Voigt profiles using commercially available peak fitting software. The integrated intensities of seven characteristic peaks (at 15.7°, 16.0°, 17.0°, 17.4°, 17.5°, 18.9°, and 19.3° 2 θ) for the crystalline Compound 1 were summed. A linear regression was applied to the relative intensity as a function of percent crystallinity. For the baseline intensity standard curve, the powder patterns were smoothed with five-point moving averages. To account for background X-ray scattering contribution from the sample holder, the diffraction from an empty sample holder was collected. The background intensity was subtracted from the baseline intensity of each powder pattern. A second standard curve was generated using the sum of the baseline intensities at 15.2°, 16.5°, 18.4°, and 19.9° 2 θ , where crystalline Compound 1 does not diffract.

Results and discussion

As the samples were prepared from hexane slurries, the possibility of recrystallization and hence change of crystallinity of Compound 1 in hexane needs to be ruled out. After the 0% crystalline Compound 1 sample was prepared in hexane slurry, the HPLC analysis of the supernatant resulted in 200 ppm of Compound 1 in hexane. With such low solubility, slurring Compound 1 in hexane is believed to have resulted in minimal recrystallization.

¹⁹F solid-state NMR

The ¹⁹F solid-state NMR spectra of four standard blends of Compound 1 (100%, 50%, 25%, and 0% crystalline) and the crushed tablets are shown in Figure 1. As expected, the full width at half maximum of the crystalline peak is smaller when compared to that of the amorphous peak (because the amorphous material samples all possible orientations). Accordingly, the ¹⁹F resonance peak broadens as the amorphous content of the blends increases. As the full width at half maximum of the ¹⁹F resonance of crushed tablets is between that of 50% and 100% crystalline Compound 1, the crystallinity of the crushed tablets is estimated to be somewhere between 50% and 100%.

The ¹⁹F T_1 spin-lattice relaxation data on the crystalline–amorphous mixtures and the crushed tablets were obtained using an inversion recovery sequence. The crystalline material has a ¹⁹F T_1 of 2.17 s while the amorphous material has a T_1 of 1.33 s. It is typical for the amorphous material to have a lower T_1 value when compared to the crystalline material as it has more relaxation avenues¹⁸. This difference in T_1 relaxation

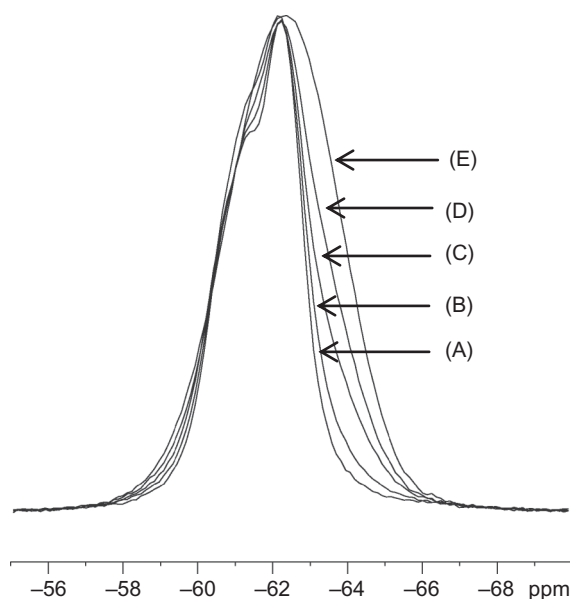


Figure 1. ^{19}F NMR spectra of (A) 100%, (C) 50%, (D) 25%, (E) 0% crystalline Compound 1, and (B) crushed Compound 1 tablets.

times between the crystalline and amorphous materials can be exploited for amorphous quantification. Typically, biphasic systems are expected to display biexponential relaxation behavior if there is no phase mixing in the system. It is reasonable to assume the mixtures are phase separated when considering blends of crystalline and amorphous phases as crystallization leads to phase separation. Figure 2 shows the experimental relaxation curve of the crushed tablet fitted to a biexponential relaxation model ($R^2 = 0.998$) using the T_1

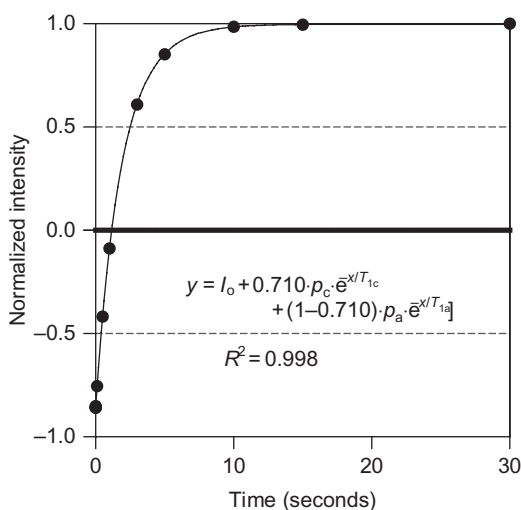


Figure 2. T_1 relaxation curve of the crushed Compound 1 tablets. Data are fitted to a biexponential curve with the parameters from the pure crystalline and amorphous fitting ($I_o = .999$, $T_{1c} = 2.17$, $p_c = -1.84$, $T_{1a} = 1.33$, $p_a = -1.82$).

relaxation rates calculated for the pure crystalline and the pure amorphous material. The crystallinity of crushed tablets was determined to be $71.0 \pm 2.6\%$. The error in the calculated crystallinity was propagated from the error based on signal-to-noise ratio analysis and the standard errors of the fitted parameters.

A model-independent method was also used to quantify the crystallinity of Compound 1 in the crushed tablets. Figure 3 shows the T_1 relaxation curves of amorphous and crystalline Compound 1 in the range of 0–3 seconds delay time. It is clear from Figure 3 that the crystalline signal is zero at T_1 delay of 1.31 s (marked with an arrow) while there is still significant signal intensity from the amorphous phase. Therefore, if the delay time τ is set to 1.31 s in the inversion recovery experiment, the signal attributed to the crystalline phase will be turned off and only amorphous signal will be detected. Figure 4 shows the ^{19}F spectra of the 100%, 50%, 25%, and 0% crystalline blends and the crushed tablets using an inversion recovery sequence with the delay set to 1.31 seconds. The crystallinity of the compacted tablets can then be calculated by direct integration of the amorphous standard and the crushed tablets after correction for the weight of sample used in the experiments. The 50% crystalline standard blend serves as validation; its crystallinity from this method is calculated as 51.7%. The crystallinity value of the crushed tablets using this method was calculated as $72.3 \pm 1.1\%$, which is in good agreement with the ^{19}F T_1 calibration curve-based method. On a different note, the solid-state NMR methods described here can be used even in the presence of excipients as ^{19}F nucleus is selectively being probed.

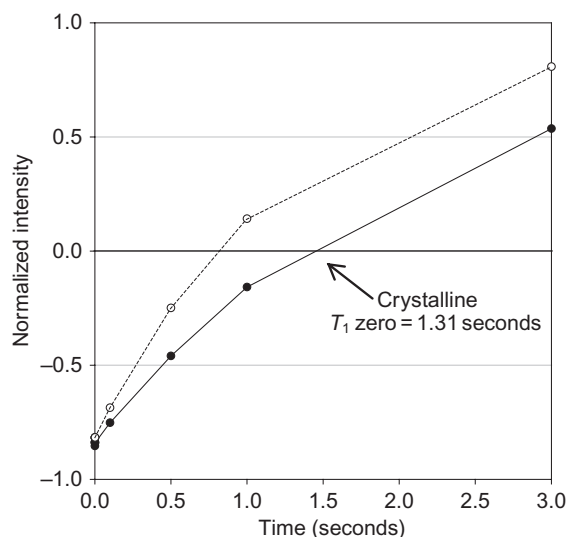


Figure 3. T_1 relaxation curves of amorphous (open circles) and crystalline (solid circles) Compound 1 in the range of 0–3 seconds delay time.

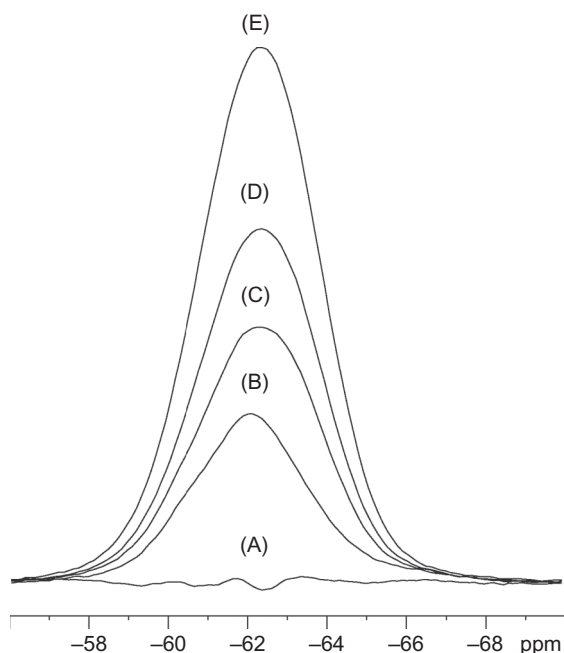


Figure 4. ^{19}F spectra of (A) 100%, (C) 50%, (D) 25%, and (E) 0% crystalline blends and (B) crushed tablets at 1.31 seconds delay time.

X-ray diffraction

The X-ray diffraction pattern of the crystalline Compound 1 from 4° to 40° 2θ is shown in Figure 5. For quantitative analysis of the amorphous content in compacted tablets, calibration curves were obtained using blends of known weight fractions of the crystalline phase. In binary systems consisting of crystalline and amorphous phases of the same compound, the diffraction intensity is linearly related to the concentration of the crystalline phase. A calibration curve can be obtained by plotting the diffracted intensity of the standard blends as a function of the weight fraction of the crystalline phase. As peak intensity is used for the calibration curve, two major sources of undesirable intensity fluctuations, microabsorption, and preferred orientation, need to be reduced. The microabsorption effect is addressed through controlling the particle size of the powder samples. Preferred orientation error is reduced by measuring the diffraction in triplicate as well as using the sum of integrated intensities from several diffraction peaks. In Figure 5, the range from 15° to 20° 2θ contains six to seven intense diffraction peaks and is therefore a suitable range for data collection. The powder diffraction patterns of 100%, 95%, 90%, 85%, 75%, 50%, 25%, and 0% crystalline Compound 1 standard blends from 15° to 20° 2θ are shown in Figure 6. There are seven intense diffraction peaks for the 100% crystalline sample, at 15.7° , 16.0° , 17.0° , 17.4° , 17.5° , 18.9° , and 19.3° 2θ . These seven reflections were fitted to a pseudo-Voigt¹⁹ profile to

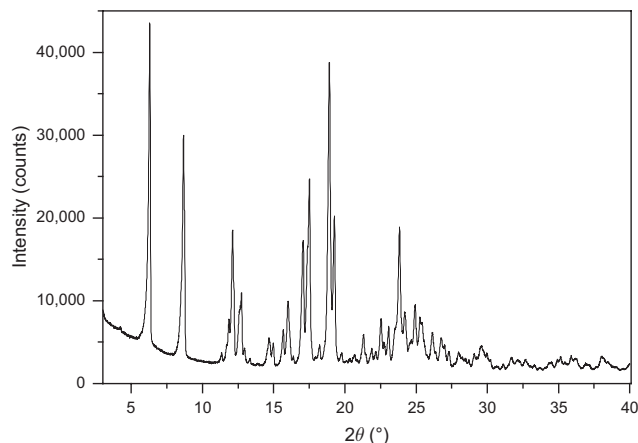


Figure 5. X-ray diffraction powder pattern of crystalline Compound 1 from 4° to 40° 2θ .

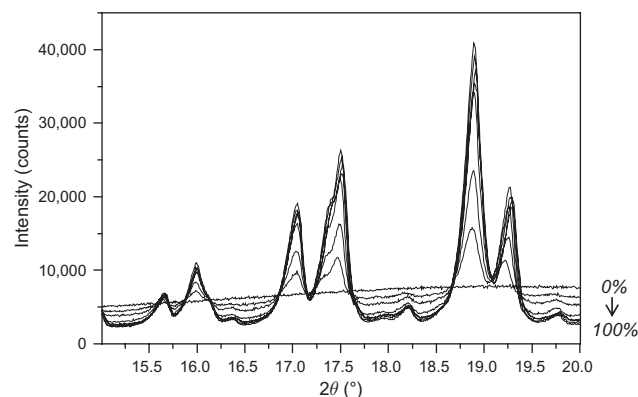


Figure 6. X-ray diffraction patterns of blends of crystalline and amorphous Compound 1.

obtain the integrated intensity. The calibration curve in Figure 7 shows the relative sum of the integrated intensities of the seven peaks averaged over three scans (relative standard deviation less than 6%) plotted as a function of the percent crystallinity. A linear calibration curve of the relative intensity (y) as a function of the percent crystallinity (x) yields a regression equation with a correlation coefficient of 0.999.

The coherent scattering from the amorphous phase of the standard blends in Figure 6 gives rise to a diffuse 'halo.' The intensity of the amorphous halo corrected from the background is related to the concentration of the amorphous phase in exactly the same manner as the intensity of the diffraction peaks is related to the concentration of the crystalline phase. The maximum of the halo for an amorphous material is dependant on the radial distribution of the material and is usually in the range between 15° and 30° 2θ . In the case of Compound 1, the maximum of the amorphous halo is around 20° 2θ . The X-ray diffraction data in Figure 6 was measured in

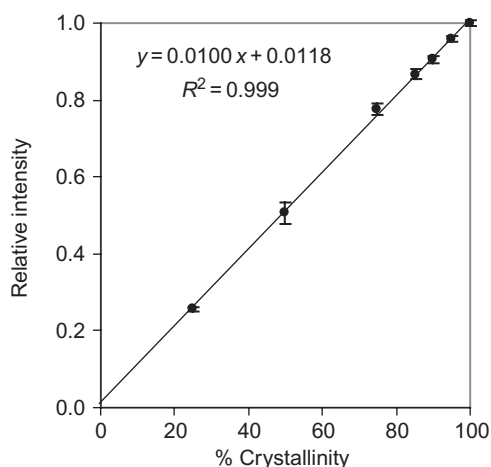


Figure 7. Relative integrated X-ray diffraction intensity of selected peaks of Compound 1 as a function of percent crystallinity. Data are fitted to a linear curve using a least-squares method. Standard deviations are represented by vertical bars ($n = 3$).

the range of 15° to 20° 2θ , which covers part of the amorphous halo and is suitable for obtaining a calibration curve using the intensity of the amorphous halo. Four 2θ positions were identified on scattered amorphous halo without interference from the crystalline phase: 15.2° , 16.5° , 18.4° , and 19.9° 2θ . The sum of the intensities at these four positions was averaged over three measurements (relative standard deviation less than 3%) and was plotted against the weight fraction of crystalline Compound 1. Figure 8 shows the linear calibration curve of the intensity (y , counts) as a function of the percent crystallinity (x) with a correlation coefficient of 0.999.

The two X-ray calibration curves are obtained from triplicate measurements with small standard deviations

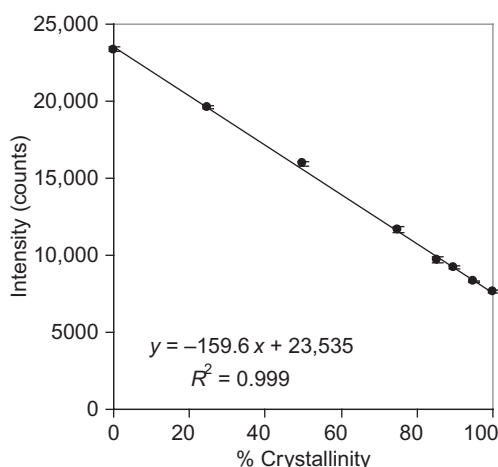


Figure 8. Intensity of X-ray scattered by amorphous Compound 1 as a function of percent crystallinity. Data are fitted to a linear curve using a least-squares method. Standard deviations are represented by vertical bars ($n = 3$).

and are linear with high correlation coefficients. The extent of the compaction-induced crystallinity reduction for Compound 1 was analyzed using these two standard curves. The crystallinity of compacted tablets was determined to be $75.9 \pm 1.8\%$ from the diffracted peak method and $75.0 \pm 1.7\%$ from the amorphous halo method. The error in the calculated crystallinity was propagated from triplicate measurements and the standard errors of the calibration curve parameters. Percent crystallinity from both calibration methods are in excellent agreement with each other and with ^{19}F solid-state NMR calculated values.

Conclusions

Solid-state ^{19}F NMR is shown to be a powerful technique to determine the percent crystallinity of Compound 1, a fluorine-containing pharmaceutical solid, after compaction. ^{19}F T_1 relaxation-based methods involving two reference standards and another using one reference standard resulted in similar percent crystallinity for the compacted Compound 1. These results were confirmed by the more traditional technique of X-ray diffraction, in which two calibration curves were obtained from the intensity of diffracted peaks and the amorphous halo. The combination of multiple methods and techniques provides higher confidence in the quantification results. With the increasing number of fluorine-containing pharmaceutical compounds in development, solid-state ^{19}F NMR is a useful and reliable amorphous quantification technique for pharmaceutical scientists.

Acknowledgments

We thank Yong Xie for providing the compacted tablets as well as useful discussion. We are grateful to Drs Shawn Walker and Margaret Faul for providing the active pharmaceutical ingredient. The support from the Amgen Small Molecule Pharmaceutical R&D Department is greatly appreciated.

Declaration of interest: The authors report no conflicts of interest.

References

1. Yu L. (2001). Amorphous pharmaceutical solids: Preparation, characterization and stabilization. *Adv Drug Deliv Rev*, 48(1):27–42.
2. Hancock BC, Zografi G. (1997). What is the true solubility advantage for amorphous pharmaceuticals? *J Pharm Sci*, 86(1):1–12.
3. Nakai Y, Fukuoka E, Nakajima S, Hasegawa J. (1977). Crystallinity and physical characteristics of microcrystalline cellulose. *Chem Pharm Bull*, 25(1):96–101.

4. Pikal MJ, Lukes AL, Lang JE, Gaines K. (1978). Quantitative crystallinity determinations for beta-lactam antibiotics by solution calorimetry: Correlations with stability. *J Pharm Sci*, 67(6):767-73.
5. Saleki-Gerhardt A, Ahlneck C, Zografi G. (1994). Assessment of disorder in crystalline solids. *Int J Pharm*, 101(3):237-47.
6. York P. (1983). Solid-state properties of powders in the formulation and processing of solid dosage forms. *Int J Pharm*, 14(1):1-28.
7. Ahlneck C, Zografi G. (1990). The molecular basis of moisture effects on the physical and chemical stability of drugs in the solid state. *Int J Pharm*, 62(2-3):87-95.
8. Burt HM, Mitchell AG. (1981). Crystal defects and dissolution. *Int J Pharm*, 9(2):137-52.
9. Klug HP, Alexander LE. (1974). X-ray diffraction procedures for polycrystalline and amorphous materials. New York: Wiley.
10. Buckton G, Darcy P. (1999). Assessment of disorder in crystalline powders—A review of analytical techniques and their application. *Int J Pharm*, 179(2):141-58.
11. Shah B, Kakumanu VK, Bansal AK. (2006). Analytical techniques for quantification of amorphous/crystalline phases in pharmaceutical solids. *J Pharm Sci*, 95(8):1641-65.
12. Harris RK. (2007). Applications of solid-state NMR to pharmaceutical polymorphism and related matters. *J Pharm Pharmacol*, 59(2):225-39.
13. Tishmack PA, Bugay DE, Byrn SR. (2003). Solid-state nuclear magnetic resonance spectroscopy—pharmaceutical applications. *J Pharm Sci*, 92(3):441-74.
14. Gustafsson C, Lennholm H, Iverson T, Nystrom C. (1998). Comparison of solid-state NMR and isothermal microcalorimetry in the assessment of the amorphous content of lactose. *Int J Pharm*, 174(1-2):243-52.
15. Lefort R, De Gussemme A, Willart JF, Danede F, Descamps M. (2004). Solid state NMR and DSC methods for quantifying the amorphous content in solid dosage forms: An application to ball-milling of trehalose. *Int J Pharm*, 280(1-2):209-19.
16. Offerdahl TJ, Salsbury JS, Dong Z, Grant DJ, Schroeder SA, Prakash I, et al. (2005). Quantitation of crystalline and amorphous forms of anhydrous neotame using ^{13}C CPMAS NMR spectroscopy. *J Pharm Sci*, 94(12):2591-605.
17. Wenslow RM. (2002). ^{19}F solid-state NMR spectroscopic investigation of crystalline and amorphous forms of a selective muscarinic M_3 receptor antagonist, in both bulk and pharmaceutical dosage form samples. *Drug Dev Ind Pharm*, 28(5):555-61.
18. Aujla RS, Harris RK, Packer KJ, Parameswaran M, Say BJ, Bunn A, et al. (1982). Discriminatory experiments in high-resolution ^{13}C NMR of solid polymers. *Polym Bull*, 8:253-9.
19. Thompson P, Cox DE, Hastings JB. (1987). Rietveld refinement of Debye-Scherrer synchrotron X-ray data from alumina. *J Appl Crystallogr*, 20(2):79-83.

Copyright of Drug Development & Industrial Pharmacy is the property of Taylor & Francis Ltd and its content may not be copied or emailed to multiple sites or posted to a listserv without the copyright holder's express written permission. However, users may print, download, or email articles for individual use.